Appendix S2: Viral Production Estimates from BONCAT

1. Viral BONCAT – Image analysis

Incorporation of HPG by viruses was quantified from these digital images by measuring the fluorescence signal of the azide-containing TAMRA fluorophore (i.e., click signal in Cy3) relative to the fluorescence signal from the SYBR Gold (i.e., DNA signal in FITC) within individual viral particles. Matlab code used for image analysis can be downloaded from GitHub (https://github.com/apasulka/Viral-BONCAT).

2. Viral BONCAT - Theoretical approach

In an effort to constrain the precision of our estimates of newly synthesized viruses, we coupled a rank-sum test with a bootstrap approach. Using a rank sum test, we determined the probability that a random sample drawn from the HPG positive treatment has greater R:G values than a random sample drawn from the HPG negative treatment, and vice versa (*P(pos>neg)* and *P(neg>pos)*, respectively). The viral activity underlying the shift from lower to higher R:G values in response to HPG is captured by the difference between *P(pos>neg)* and *P(neg>pos)*. By simulating repeated draws from these distributions (bootstrap resampling with 1000 trials), we estimate confidence intervals for these activity estimates. This approach assumes independence between the viral particles measured in the compared samples (i.e., no direct link between particles), and requires that viral activity in the presence of HPG leads to a positive shift in observed R:G fluorescence intensity ratios. The sensitivity of this method to the degree of R:G shift is explored in more detail below.

3. Viral BONCAT - Sensitivity testing

We modeled the number of methionine substitutions from a binomial distribution with a specified expected value (i.e., the average number of substitutions; $E[X] = np$). Code to reproduce the modeling results can be found at downloaded from GitHub (https://github.com/apasulka/Viral-BONCAT). Using the known number of methionine sites for T7, Syn1 and EhV207 as well as two

synthetic viruses (tiny and huge), we explored the impact of the number of substitution sites (n) and the probability of substitution (*p*) on the binomial probability distribution. Figs. 1 and 2 illustrate that variations in n and *p* influence the shape of the probability distribution, but only when there are a relatively small number of methionine sites or high substitution probabilities. For relative small substitution probabilities (<10%) and/or large proteomes relative to the average number of substitutions (>400 sites, i.e., T7), the probability density functions are almost identical and were therefore treated as such for modeling (i.e., the average number of substitutions in the only real free parameter).

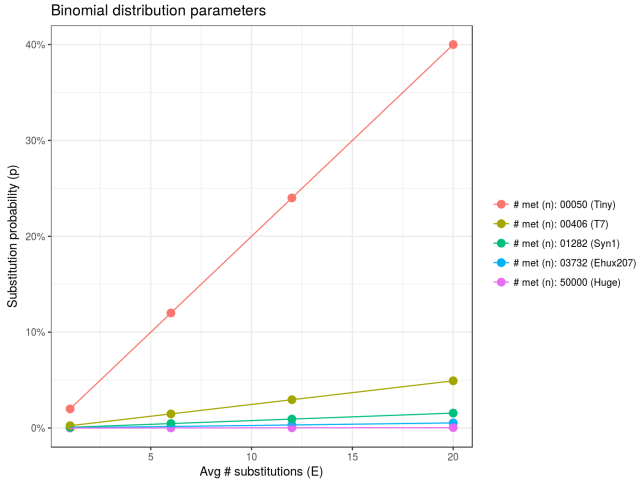

Figure 1.

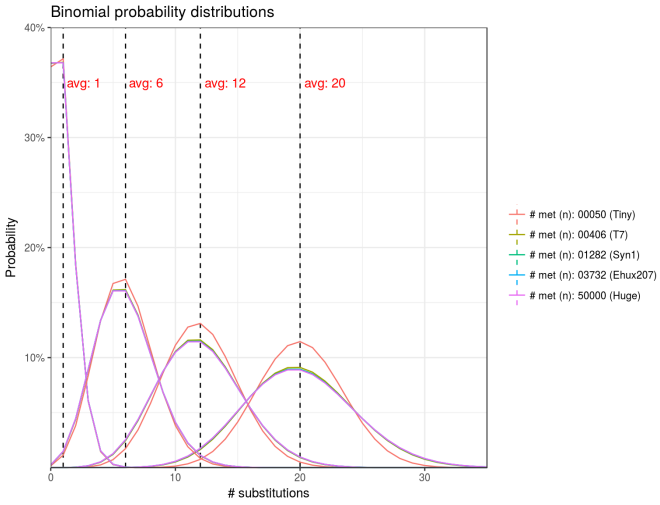

Figure 2.

The number of detected substitutions and the impact of an HPG substitution on the R:G ratio were estimated from T7 data (12 and 0.0491, respectively). However, depending on where the substitution sites are located and how large the viral particles are, these parameters may vary and therefore we modeled several values for these parameters. We simulated the production of new viruses (termed % active for the purposes of modeling) by adding a random number of methionine substitutions (modeled with a binomial distribution each increasing the R:G amount) to a subset (x percent) of the negative control R:G ratios with a different number of particles

in play. Using 1000 particles drawn from the T7 negative control distribution, we explored how the following conditions impacted the probability distributions of HPG-labeled particles: n_{subs} = 1, 5, 12; *d*RG = 0.01, 0.03, 0.05; % active = 5, 25, 50, 75, 100. In an effort to model the variability that individual substitutions may have on the actual changes in R:G, we also explored how percent variations in *d*RG (± % of the average *d*RG) for individual substitutions influenced the probability distributions of HPG-labeled viruses. For example, if *d*RG = 0.05 and the range is +/-60%, then each substitution will randomly cause a change in R:G between 0.02 (0.05-0.6*0.05) and 0.08 (0.05+0.6*0.05).

4. Viral production calculations

Viral production rates were calculated using the equations from Noble and Fuhrman (2000), but rather than track the disappearance of fluorescently labeled viruses, we essentially tracked the disappearance of unlabeled viruses as fluorescently labeled viruses were produced.

The decay constant, k, was calculated as k = [ln (R_0/R_t)/t], where t is incubation time and R_0 and R_t are the ratios of unlabeled viruses (ULV_0) to the total virus abundance at time zero and time t, respectively. The mean specific activity, R, was calculated as

(1) $R = \frac{R_0}{k\ x\ t} \times 1 - \ e^{-kt}$.

The viral decay or removal rate, D_v, was then calculated as

(2) $Dv = \frac{ULV_0 - ULV_t}{R\ x\ t}$,

where ULV_0 and ULV_t are the concentrations of unlabeled viruses at time t_0 and time t, respectively. The viral production rate, Pv, was calculated as

(3) $Pv = \frac{\ln\left(\frac{R_0}{R_t}\right)}{\ln\left(\frac{C_0}{C_t}\right) \times t} \times (C_0 - C_t)$,

where C_0 and C_t were the total concentrations of virus particles at t_0 and time t, respectively. Viral turnover (days) was estimated by dividing the average number of viral particles by the virus production rate.

5. References

Nobel RT, Fuhrman JA (2000) Rapid virus production and removal as measured with fluorescently labeled viruses as tracers. *Appl Environ Microbiol* 66(9): 3790-3797.